

See discussions, stats, and author profiles for this publication at: <https://www.researchgate.net/publication/239717571>

# Immobilizing Au Nanoparticles on SiO<sub>2</sub> Surfaces Using Octadecylsiloxane Monolayers

ARTICLE *in* LANGMUIR · SEPTEMBER 2001

Impact Factor: 4.46 · DOI: 10.1021/la001296p

---

CITATIONS

18

---

READS

13

7 AUTHORS, INCLUDING:

[Roland Resch](#)

TU Wien

27 PUBLICATIONS 848 CITATIONS

SEE PROFILE



[Bruce Koel](#)

Princeton University

296 PUBLICATIONS 9,135 CITATIONS

SEE PROFILE



[A. Madhukar](#)

University of Southern California

380 PUBLICATIONS 10,632 CITATIONS

SEE PROFILE

# Immobilizing Au Nanoparticles on SiO<sub>2</sub> Surfaces Using Octadecylsiloxane Monolayers

Roland Resch,<sup>†</sup> Sheffer Meltzer,<sup>†</sup> Thomas Vallant,<sup>‡</sup> Helmuth Hoffmann,<sup>‡</sup>  
Bruce E. Koel,<sup>\*,†</sup> Anupam Madhukar,<sup>†</sup> Aristides A.G. Requicha,<sup>†</sup> and Peter Will<sup>†</sup>

Laboratory for Molecular Robotics, University of Southern California, 37th Street,  
University Park, Los Angeles, California 90089-0482, and Institute for Inorganic Chemistry,  
University of Technology, Getreidemarkt, A-1060 Vienna, Austria

Received September 11, 2000. In Final Form: March 27, 2001

Gold nanoparticles were immobilized on silicon dioxide (SiO<sub>2</sub>) surfaces by embedding them in a layer of octadecylsiloxane (ODS) and also in SiO<sub>2</sub> layers created by deposition and oxidation of ODS layers. The ODS and the SiO<sub>2</sub> layers form selectively around the nanoparticles. Analysis of the particles after several deposition/oxidation cycles showed a decrease in measured height in accordance with the number of deposited layers. Following one embedding cycle, the nanoparticles could not be moved with the tip of a scanning force microscope operated in dynamic mode, whereas they moved in a controlled fashion prior to the deposition of any layer. Depositing a second set of particles onto an ODS layer in contact with the substrate allowed us to construct a two-particle column by placing one particle directly on top of another one.

## 1. Introduction

The synthesis, physical characterization, and manipulation of nanometer-scale particles are very active research areas today. Nanoparticles may be synthesized out of a variety of materials,<sup>1,2</sup> in very well-defined sizes, and with a variety of properties (e.g., metallic, conductive, semiconductive, insulating, or magnetic).<sup>3–5</sup> They have potential applications that range from optoelectronic devices<sup>6</sup> to biological sensors.<sup>7</sup> For example, nanoparticles with a diameter of 1–2 nm have been proposed as a basis for future electronic digital circuits based on single-electron tunneling.<sup>8</sup> In this and many other examples, potential applications require positioning of nanoparticles in complex two- and even three-dimensional structures. Several methods ranging from self-assembly to nanomanipulation with a scanning probe microscope (SPM) have been proposed to achieve this goal.<sup>9–16</sup> A crucial issue is the

positional stability of particles on a surface, or in a structure, after they have been positioned. Surface diffusion and movement of the particles due to mechanical stress or electric field have to be eliminated.

One useful approach to particle stabilization involves the use of self-assembled monolayers (SAMs) to surround the particles. SAMs have attracted considerable interest during the last 2 decades and are formed spontaneously by immersing substrates in dilute solutions of amphiphilic molecules in appropriate solvents.<sup>17,18</sup> A variety of film/substrate systems are known to lead to the formation of these highly ordered monolayer films.<sup>19–22</sup> Among these systems, alkylsiloxane SAMs on hydroxylated surfaces have proven to be particularly versatile. These monolayers are formed from precursor molecules such as alkyltrichlorosilanes (RSiCl<sub>3</sub>), alkylaminosilanes (RSi(NR'<sub>2</sub>)<sub>3</sub>), or alkyltrialkoxysilanes (RSi(OR')<sub>3</sub>) having hydrolyzable Si<sub>x</sub> groups.<sup>23–25</sup>

Organosilane SAMs have been used in several practical applications, ranging from the modification of surface properties (e.g., wetting stability) to reactive ion-etching resists.<sup>26,27</sup> These organosilane SAMs may also play an

\* To whom correspondence should be addressed. Tel: +1-213-740-3972. Fax: +1-213-740-4126. E-mail: koel@chem1.usc.edu.

<sup>†</sup> University of Southern California.

<sup>‡</sup> University of Technology.

(1) Handley D. A. *Colloidal Gold: Principles, Methods, and Applications*; Hayat, M. A., Ed.; Academic Press: San Diego, 1989.

(2) Gorer, S.; Hsiao, G. S.; Anderson, M. G.; Stiger, R. M.; Lee, J.; Penner, R. M. *Electrochim. Acta* **1998**, *43*, 2799.

(3) Collier, C. P.; Vossmeier, T.; Heath, J. R. *Annu. Rev. Phys. Chem.* **1998**, *49*, 371 and references therein.

(4) Ni Y. H.; Ge X. W.; Xu X. L.; Chen, J. F.; Zhang, Z. C. *J. Inorg. Mater.* **2000**, *15*, 9.

(5) Gangopadhyay, R.; De, A. *Chem. Mater.* **2000**, *12*, 608 and references therein.

(6) Sato, R.; Ahmed, H.; Brown, D.; Johnson, B. F. G. *J. Appl. Phys.* **1997**, *82*, 696.

(7) Elghanian, R.; Storhoff, J. J.; Mucic, R. C.; Letsinger, R. L.; Mirkin, C. A. *Science* **1997**, *277*, 1078.

(8) Glazman, L. I. *J. Low Temp. Phys.* **2000**, *118*, 247 and references therein.

(9) Ohara, P. C.; Heath, J. R.; Gelbart, W. M. *Angew. Chem., Int. Ed. Engl.* **1997**, *36*, 1077.

(10) Perkins, F. K.; Dobisz, E. A.; Brandow, S. L.; Calvert, J. M.; Kosakowski, J. E.; Marrian, C. R. K. *Appl. Phys. Lett.* **1996**, *68*, 550.

(11) Bandyopadhyay, S.; Miller, A. E.; Chang, H. C.; Banerjee, G.; Yuzhakov, V.; Yue, D.-F.; Ricker, R. E.; Jones, S.; Eastman, J. A.; Baugher, E.; Chandrasekhar, M. *Nanotechnology* **1997**, *7*, 360.

(12) Mirkin, C. A.; Letsinger, R. L.; Mucic, R. C.; Storhoff, J. J. *Nature* **1996**, *382*, 607.

(13) Snow, E. S.; Campell, P. M.; McMarr, P. J. *Nanotechnology* **1996**, *7*, 434.

(14) Resch, R.; Baur, C.; Bugacov, A.; Koel, B. E.; Echternach, P. M.; Madhukar, A.; Montoya, N.; Requicha, A. A. G.; Will, P. *J. Phys. Chem. B* **1999**, *103*, 3647.

(15) Wilbur, J. L.; Kumar, A.; Biebuyck, H. A.; Kim, E.; Whitesides, G. M. *Nanotechnology* **1997**, *7*, 452.

(16) McCarty, G. S.; Weiss P. S. *Chem. Rev.* **1999**, *99*, 1983 and references therein.

(17) Ulman, A. *An Introduction to Ultrathin Organic Films*; Academic Press: San Diego, 1991.

(18) Ulman, A. *Chem. Rev.* **1996**, *96*, 1533.

(19) Nuzzo, R. G.; Allara, D. L. *J. Am. Chem. Soc.* **1983**, *105*, 4481.

(20) Schlotter, N.; Porter, M.; Bright, T.; Allara, D. L. *Chem. Phys. Lett.* **1986**, *132*, 93.

(21) Maoz, R.; Sagiv, J. *J. Colloid Interface Sci.* **1984**, *100*, 465.

(22) Lee, H.; Kepley, L.; Hong, H.; Mallouk, T. *J. Am. Chem. Soc.* **1988**, *110*, 618.

(23) Tripp, C. P.; Hair, M. L. *Langmuir* **1992**, *8*, 1120.

(24) Tripp, C. P.; Hair, M. L. *Langmuir* **1992**, *8*, 1961.

(25) Laibinis, P. E.; Whitesides, G. M.; Allara, D. L.; Tao, Y. T.; Parikh, A. N.; Nuzzo, R. G. *J. Am. Chem. Soc.* **1991**, *113*, 7153.

(26) Wei, M.; Bowman, R. S.; Wilson, J. L.; Morrow, N. R. *J. Colloid Interface Sci.* **1993**, *157*, 154.

(27) Li Jeon, N.; Choi, I. S.; Whitesides, G. M.; Kim, N. Y.; Laibinis, P. E.; Harada, Y.; Finnie, K. R.; Girolami, G. S.; Nuzzo, R. G. *Appl. Phys. Lett.* **1999**, *75*, 4201.

important role in the construction of future electronic devices because the hydrocarbon chain can be oxidized and removed by a combined UV/ozone exposure to form an ultrathin film of silicon dioxide (SiO<sub>2</sub>). A controlled, layer-by-layer growth can be achieved because of the self-limiting nature of the organosilane deposition.<sup>28</sup>

In this paper, we present a strategy to immobilize gold nanoparticles on SiO<sub>2</sub> surfaces by embedding them into a layer of octadecylsiloxane (ODS) and multiple layers of SiO<sub>2</sub> created by deposition and hydrocarbon oxidation of ODS SAMs. This strategy was used to construct a two-particle column by first depositing and embedding a set of particles and then depositing a second set of particles and placing one of these by directed nanomanipulation on top of a previously embedded particle.

## 2. Experimental Section

Colloidal gold particles (EM.GC15, Ted Pella Inc.) with a nominal diameter of 5 nm were chemically modified with hexanethiol and transferred to a toluene phase. A 2  $\mu$ L portion of dodecanthiol was added to a two-phase system of 10 mL of aqueous, colloidal solution and 10 mL of toluene. After the flask was shaken for 2 min, the red color of the aqueous phase was transferred to the organic phase indicating the replacement of the chloride ion shell of the gold particles by a nonpolar thiol shell. Subsequently, a 10  $\mu$ L gold particle solution was added to the two-phase system to minimize the amount of "free" thiols in the organic phase. Treatment with hexanethiol changed<sup>13,29,30</sup> the average diameter of the particles to approximately  $5.4 \pm 1.4$  nm as determined by scanning force microscope (SFM) height measurements.<sup>31</sup> In general, the size uniformity of the particles changes and the average particle size exhibits a larger deviation than the original, chlorine-stabilized particles (coefficient of variation <15% as analyzed by the manufacturer). The modification of particles following this recipe also results in the formation of agglomerates of particles in solution, and the appearance of agglomerates becomes pronounced with time (due to "aging of the solution"). Therefore, a fresh solution of thiolated colloids, usually diluted by a factor of 20–50, was prepared before every experiment.

The Si substrates were treated prior to deposition in an UV/ozone chamber for 15 min to ensure a sufficiently thick, clean SiO<sub>2</sub> layer for silane deposition. Subsequently, a drop of 10  $\mu$ L of the particle solution was placed onto the Si/SiO<sub>2</sub> substrates and the toluene was evaporated. After evaporation of the solvent, the samples were rinsed with an excess of toluene and "blow-dried" with nitrogen. The deposition of ODS was achieved by immersing the substrates into a  $5 \times 10^{-4}$  M solution of octadecyltrichlorosilane (OTS, Aldrich, 95%) in toluene. Subsequently, the samples were rinsed with toluene, acetone, and ethanol and then dried in a stream of pure nitrogen. The ODS layer on the sample was subsequently oxidized by exposure in an UV/ozone chamber for 10 min.

Imaging and manipulation experiments were carried out by using an Autoprobe CP atomic force microscope (AFM) (Park Scientific Instruments) operated in a dynamic mode in air using triangularly shaped silicon cantilevers (Park Scientific Instruments,  $13.0 \text{ N m}^{-1}$  spring constant, and 340 kHz resonance frequency). The setup that we use for nanomanipulation with a SFM has been previously described.<sup>32–34</sup> It is based on Probe

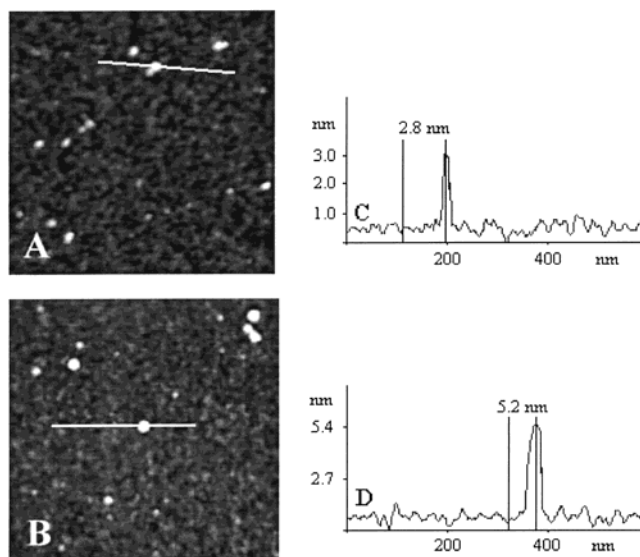


**Figure 1.** Sequence of  $500 \times 500 \text{ nm}^2$  SFM images displaying areas of a SiO<sub>2</sub>/nanoparticle sample: A, after deposition of an ODS layer; B, after oxidation of the hydrocarbon present in ODS. The change in the height of the particles is displayed in the corresponding linescans C and D. The scan size is  $1 \times 1 \mu\text{m}^2$  and the height scale in the images is (A) 2 nm and (B) 3.5 nm from black to white, respectively.

Control Software (PCS) developed in our group and built upon the application programming interface (API) provided by PSI.

## 3. Results and Discussion

Gold nanoparticles were initially deposited in a random manner at a low coverage (density) on the SiO<sub>2</sub> substrate. Although there are techniques known for the deposition of gold particle monolayers<sup>37,38</sup> and multilayers<sup>39</sup> with controlled interparticle distances on derivatized surfaces, the interparticle distance is largely irrelevant for our purposes except that a low density is crucial for precise manipulation.

Because the particles are electrically neutral and no adhesive layer is used,<sup>35,36</sup> there is no chemical or electrostatic interaction between the substrate and the particle, i.e., they are physisorbed on the surface. Close-packed arrays of alkanethiol-capped gold nanoparticles on a "naked" SiO<sub>2</sub> substrate have been shown to be mechanically stable.<sup>40</sup> However, as a result of the weak interaction between the substrate and single particles in experiments, imaging with the SFM even in dynamic mode requires carefully selected setup parameters.<sup>41</sup>

The randomly deposited gold nanoparticles had a height of  $\sim 5.4 \pm 1.5$  nm as measured by the SFM (images not shown). Figure 1 shows SFM images of the sample after deposition of an ODS layer, panel A and after oxidation of the ODS layer by a UV/ozone treatment for 10 min, panel B. The scan area was  $500 \times 500 \text{ nm}^2$  in both images.

(28) Brunner, H.; Vallant, T.; Mayer, U.; Hoffmann, H. *Langmuir* **1996**, *12*, 4614.

(29) Laibins, P. E.; Nuzzo, R. G.; Whitesides, G. M. *J. Phys. Chem.* **1992**, *96*, 5097.

(30) Terrill, R. H.; Postlethwaite, T. A.; Chen, C.-H.; Poon, C.-D.; Terzis, A. *J. Am. Chem. Soc.* **1995**, *117*, 12537.

(31) Grabar, K. C.; Brown, K. R.; Keating, C. D.; Stranick, S. J.; Tang, S.-L.; Natan, M. J. *Anal. Chem.* **1997**, *69*, 471.

(32) Resch, R.; Bugacov, A.; Baur, C.; Gazen, B. C.; Koel, B. E.; Madhukar, A.; Requicha, A. A. G.; Will, P. *Appl. Phys. A* **1998**, *67*, 265.

(33) Resch, R.; Baur, C.; Bugacov, A.; Koel, B. E.; Madhukar, A.; Requicha, A. A. G. *Langmuir* **1998**, *14*, 6613.

(34) Baur, C.; Bugacov, A.; Koel, B. E.; Madhukar, A.; Montoya, N.; Ramachandran, T. R.; Requicha, A. A. G.; Resch, R.; Will, P. *Nanotechnology* **1998**, *9*, 360.

(35) Andres, R. P.; Bielefeld, J. D.; Henderson, J. I.; Janes, D. B.; Kolagunta, V. R.; Kubiak, C. P.; Mahoney, W. J.; Osifchin, R. G. *Science* **1996**, *273*, 1690.

(36) Gutierrez-Wing, C.; Santiago, P.; Ascencio, J. A.; Camacho, A.; Jose-Yacamán, M. *Appl. Phys. A* **2000**, *71*, 237.

(37) Musick, M. D.; Grabar, K. C.; Smith, P. C.; Davis, J. A.; Walter, D. G.; Jackson, M. A.; Guthrie, A. P.; Natan, M. J. *J. Am. Chem. Soc.* **1996**, *118*, 1148.

(38) Doron, A.; Katz, E.; Villner, I. *Langmuir* **1995**, *11*, 1313.

(39) Musick, M. D.; Pena, D. J.; Botsko, S. L.; McEvoy, T. M.; Richardson, J. N.; Natan, M. J. *Langmuir* **1999**, *15*, 844.

(40) Tsutsui, G.; Huang, S.; Sakaue, H.; Shingubara, S.; Takahagi, T. *Jpn. J. Appl. Phys.* **1999**, *38*, L1488.

(41) Rolandi, M.; Scott, K.; Wilson, E. G.; Meldrum, F. C. *J. Appl. Phys.* **2001**, *89*, 1588.



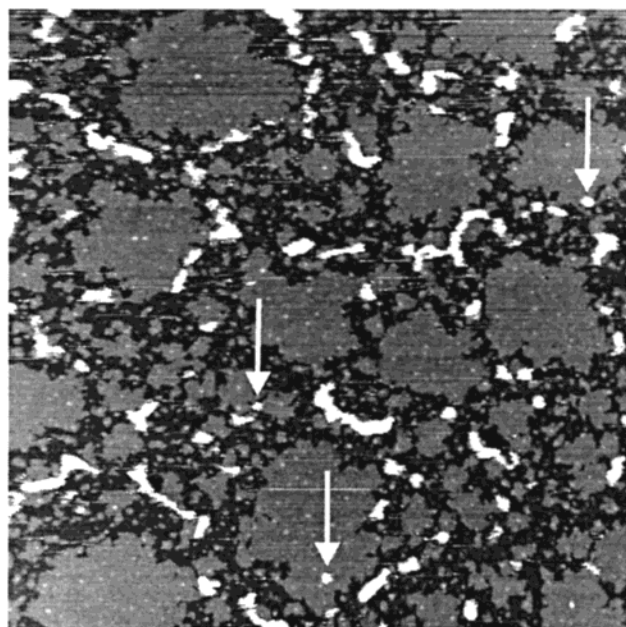


**Figure 2.** SFM image showing the effect of OTS deposition on a nanoparticle/SiO<sub>2</sub> substrate in high humidity (80%) conditions. This image reveals large islands of ODS and agglomerations of particles in areas where no ODS was deposited. The arrows mark individual particles that were found in areas where ODS was present.

Figure 1A shows an area of the sample which is completely covered with an ODS layer. The linescan in Figure 1C indicates that the height measured for the particles above the coated substrate decreased to  $2.8 \pm 1.0$  nm. This is consistent with our other experiments, since the height of one monolayer of ODS is  $\sim 2.7$  nm.<sup>28,42</sup> Parts B and D of Figure 1 show that the measured height of the particles increased to  $5.2 \pm 1.3$  nm after hydrocarbon oxidation of the ODS layer. Again, this result is as expected, because the thickness of one layer of SiO<sub>2</sub> is  $\sim 2.75$  Å.<sup>24</sup> Furthermore, the fact that these particles could not be moved subsequently by SFM manipulation indicates that they were embedded in a SiO<sub>2</sub> layer generated by the oxidation treatment.

To ensure that the  $\sim 5$  nm features in Figure 1 were not OTS aggregates, we used the same deposition procedure to deposit an ODS monolayer on a clean Si substrate without gold nanoparticles on it. The modified substrate was analyzed by contact angle measurements to show that the SAM deposition took place. We imaged the sample by using the SFM (images not shown) after the ODS deposition, and we did not see any nanometer-scale features on the substrate. These results are also supported by the previous work by Vallant et al.<sup>42</sup> and Resch et al.<sup>43</sup> who investigated the ODS/Si system using SFM, IR, and ellipsometry in situ and ex situ.

Special consideration has to be given to sample preparation, e.g., to the amount of surface water and water content of the OTS solution. Recently, it has been shown that the deposition of ODS is influenced by the amount of water in the solution.<sup>42</sup> In general, higher water content leads to the deposition of larger islands of ODS. The same trend was observed with the deposition of the ODS layer on a SiO<sub>2</sub> surface in high humidity. Figure 2 shows a SFM image of a nanoparticle/SiO<sub>2</sub> substrate treated with OTS

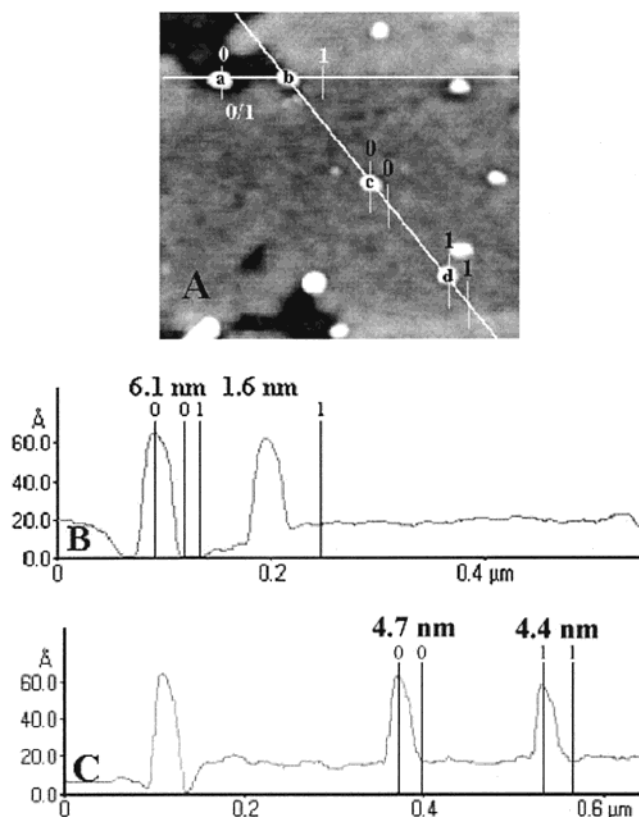


**Figure 3.** SFM image, A, and corresponding line scans, B and C, recording the embedding of Au nanoparticles in layers of SiO<sub>2</sub> by successive ODS deposition and oxidation cycles. The maximum height difference between uncovered and covered areas was measured to be 1.6 nm, corresponding to six layers of SiO<sub>2</sub>. The scan size is  $500 \times 500$  nm<sup>2</sup>, and the height scale is 3 nm from black to white.

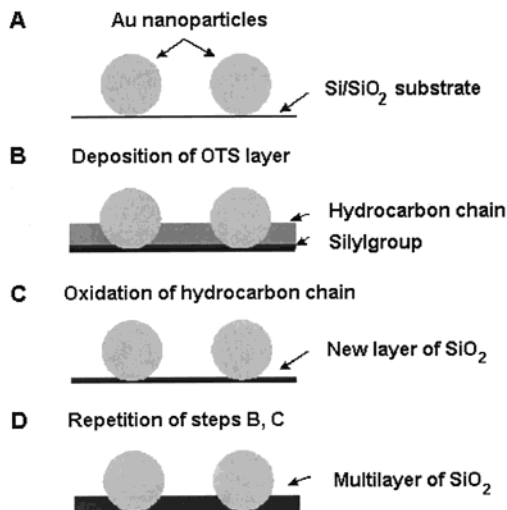
for 40 s in 80% humidity. This image reveals large islands of ODS and agglomerations of particles in areas where no ODS was deposited. Very few individual particles were found in areas where ODS was present (as marked by the arrows), and the density of particles decreased as well. This indicates that most of the nanoparticles were displaced from their original positions by the deposition and formation of large ODS islands.

Figure 3A shows a SFM image of an Au-nanoparticles/SiO<sub>2</sub> sample that has undergone six ODS deposition/oxidation cycles according to Chart 1. In each cycle, the sample was immersed in the OTS deposition solution for 2 h. The area displayed was found close to the edge of the Si substrate where the ODS deposition was not homogeneous, probably because of handling of the substrate between cycles. In these areas the thickness of the oxidized ODS layer on the original SiO<sub>2</sub> can be measured. The height of the layer according to the line scan displayed in Figure 3B was 1.6 nm, in good agreement with the expected thickness of 1.65 nm, i.e., 6 times the thickness of one layer of SiO<sub>2</sub> ( $2.75$  Å<sup>24</sup>). The particles marked as "a" and "b" are located in an "uncovered" area and exhibit the same height of  $\sim 6.0$  nm. Particle b is close to the edge of the deposited SiO<sub>2</sub>. The particles marked as "c" and "d" are located in the middle of this layer and have a height of  $\sim 4.5$  nm as shown in the line scan displayed in Figure 3C.

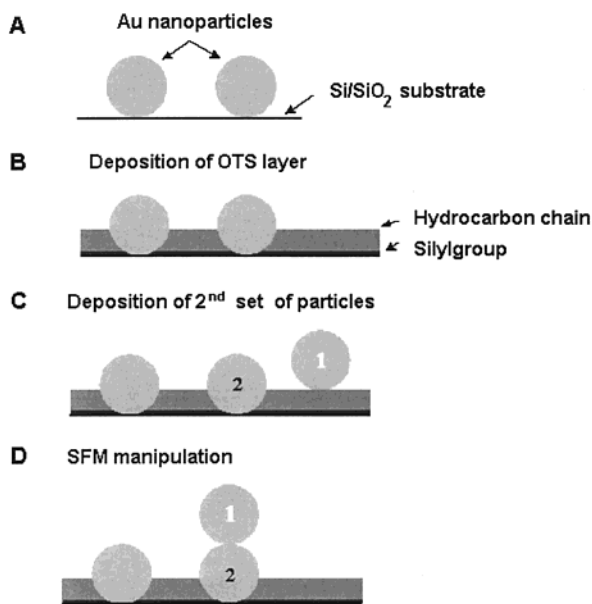
Additionally, the growth of the ODS layer was monitored with external reflection infrared spectroscopy and ellipsometry. Results from these studies are given in Table 1 and reveal a uniform layer-by-layer growth with each deposition/oxidation cycle. Previously, Brunner et al.<sup>28</sup>

(42) Vallant, T.; Brunner, H.; Mayer, U.; Hoffmann, H.; Leitner, T.; Resch, R.; Friedbacher, G. *J. Phys. Chem. B* **1998**, *102*, 7190.

(43) Resch, R.; Grasserbauer, M.; Friedbacher, G.; Vallant, T.; Brunner, H.; Mayer, U.; Hoffmann, H. *Appl. Surf. Sci.* **1999**, *140*, 168.

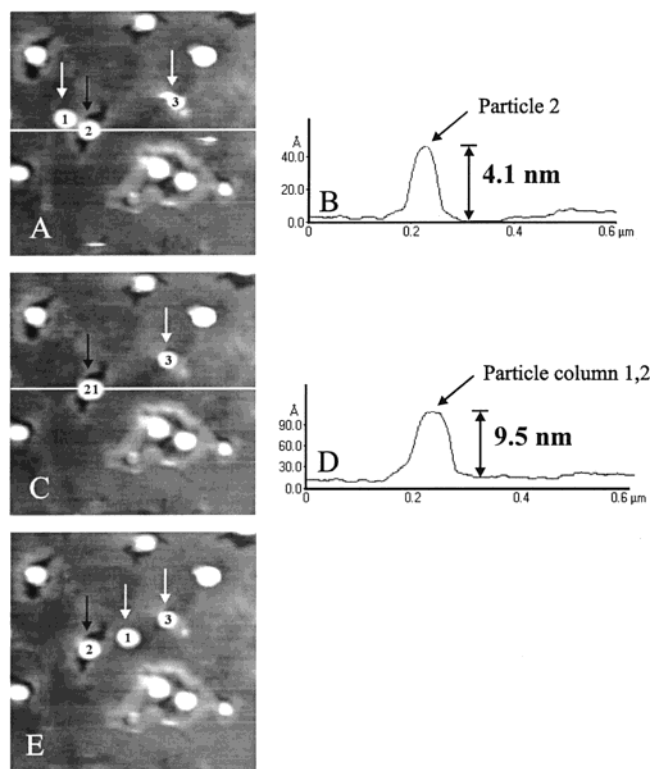
**Chart 1. Schematic View of the Embedding Procedure of Nanoparticles in a SiO<sub>2</sub> Matrix As Presented in Figure 3****Table 1. Thickness of SiO<sub>2</sub> Layers after Several Successive Deposition/Oxidation Cycles As Measured by Ellipsometry**

no. of dephn/ oxidn cycles	thickness of SiO <sub>x</sub> layer (Å)	increase in thickness of SiO <sub>x</sub> layer (Å)
0	19.2	
1	21.9	2.7
2	24.4	2.5
3	27.5	3.1
4	30.5	3.0
5	33.4	2.9
6	36.1	2.7
		Σ = 16.9

**Chart 2. Schematic View of the Construction of a Two-Particle, Upright Column As Displayed in Figure 4**

grew SiO<sub>2</sub> films with complete and uniform layer-by-layer growth using up to 23 deposition/oxidation cycles.

In principle, it should be possible to build 3-D nanostructures by using a strategy of embedding and immobilizing nanoparticles. Chart 2 illustrates the construction of a vertical column by utilizing layers of particles. Figure 4 shows a demonstration experiment along these lines. A series of SFM images show the same

**Figure 4.** SFM images and corresponding line scans displaying the successful construction of a two-particle, upright column by pushing particle "1" on top of particle "2". The scan size is 600 × 600 nm<sup>2</sup>, and the height scale is 6 nm from black to white.

area before, A, and after manipulation, C and E, of a second set of nanoparticles that was deposited onto a modified SiO<sub>2</sub> substrate containing nanoparticles and ODS. The areas where the ODS layer was not complete show a smaller film thickness. This is recorded in the SFM image in Figure 4A where a few uncovered areas of the SiO<sub>2</sub> substrate, mostly around the particles, can be observed. The particle marked "2" with the black arrow is embedded in the ODS layer, while the particles marked "1" and "3" were deposited subsequently and sit "on top" of the ODS layer. The height of particle "2" is 4.0 nm with respect to the ODS layer (Figure 4B) and 5.3 nm with respect to an uncovered area. This establishes (i) that the ODS layer was not complete because its thickness is smaller than the 2.7 nm value for a complete layer and (ii) that the particles were not substantially modified by the ODS since their height was essentially unchanged. Then, particle "1" was manipulated with the SFM and placed on top of particle "2", forming a vertical column as recorded in Figure 4C. The line scan displayed in Figure 4D gives the height of this column as 9.5 nm with respect to the ODS layer. Afterward, the particles comprising the column were again separated by manipulation, as recorded in Figure 4E.

#### 4. Concluding Remarks

The mechanical stability of nanoparticles deposited on a surface is a crucial issue for potential applications of nanoparticles as active components of future devices. The strategy presented in this paper successfully immobilizes gold nanoparticles on SiO<sub>2</sub> surfaces by embedding them in a layer of ODS. Mechanical nanomanipulation experiments with an SFM showed that the embedded particles were not movable under the same manipulation conditions that were successful prior to the embedding. Furthermore,

by exploiting the chemical selectivity of self-assembled monolayers used as anchoring layers, the simplest 3-D nanostructure, a two-particle, vertical column, was constructed. Alternatively, the gold nanoparticles can be embedded into a matrix of SiO<sub>2</sub> layers by successive ODS deposition and oxidation cycles to form stable patterns on the surface. This strategy of embedding nanostructures in a very stable matrix in combination with prior SFM nanomanipulation can be used, in principle, to construct *positive-tone* or *negative-tone nanomasks* comparable to lithography processes or as *nanomolds* for imprint techniques. With the OTS replaced with a silane molecule

containing a terminal hydroxyl group (masked, for example, as an ester group), multiple layers may be constructed. This would enable the construction of taller and more complicated nanostructures. In general, these results should not be limited to the siloxane/SiO<sub>2</sub> system. Such a strategy should work with any other appropriate substrate/particle/layer system.

**Acknowledgment.** This research was supported in part by the Z. A. Kaprielian Technology Innovation Fund and by the NSF under Grant No. EIA-98-71775.

LA001296P